Climate Vulnerability Assessment on Potential Flooding of Apponagansett Bay and Clarks Cove, Dartmouth Town, MA

Authors

Zhuo Zhang
Changsheng Chen
Robert C. Beardsley
Siqi Li
Qichun Xu

Prepared under the Dartmouth Town climate vulnerability assessment contract by
School for Marine Science and Technology
University of Massachusetts-Dartmouth
New Bedford, MA 02744

February 1, 2018

EXCUTIVE SUMMARY

The Dartmouth Town, MA has contracted the Marine Ecosystem Dynamics Modeling Laboratory (MDEM Lab), School for Marine Science and Technology (SMAST), University of Massachusetts-Dartmouth (UMASSSD) to conduct modeling experiments for the purpose of assessing the potential impacts of the climate-induced sea level rise on the storm-induced coastal inundation in the Apponagansett Bay and Clarks Cove, Dartmouth, MA. The specific objectives of this project are to 1) develop a coastal inundation sub-grid model for the Apponagansett Bay and Clark Cove, 2) select a hundred-storm scenario to estimate the potential flooding in vulnerable areas, 3) for a given same hundred-year storm condition, re-conduct the experiment with considering the climate change-induced sea level rise, and 4) create the potential flooding map in vulnerable areas under different climate change scenarios.

The change of the storm surge level along the coast of the Apponagansett Bay and Clarks Cover was controlled by the water transport inflowing from Buzzard Bay, which is driven by the tidal- and wind-induced flows through the interaction with surface waves. This region is frequently influenced by nor'easter storms during winter though spring and occasionally is struck by hurricanes. A synthesis was carried out for 364 storms that swept Buzzard Bay over the period of 1978-2016. For a hundred-year storm, the extreme wind speed reached 24 m/s (53.7 mph).

Built on the framework of the Northeast Coastal Ocean Forecast System (NECOFS), the MEDM Lab/SMAST/UMASSD has developed a high-resolution, subdomain coastal inundation model for the western Buzzard Bay coast, with the computational domain covering Apponagansett Bay and Clarks Cover. This subdomain inundation model was constructed using the unstructured grid Finite Volume Community Ocean Model (FVCOM), and named the Dartmouth Town Coastal FVCOM (abbreviated as "DTC-FVCOM"). The DTC-FVCOM was a fully coupled current-wave model system with the flooding/draining process. The computational domain covered both the water and land, and was discretized by the unstructured triangular grid with a horizontal resolution up to ~10 m. This model was driven by the tidal elevation and surface wave height on the open boundary and the surface wind at the surface.

We first used DTC-FVCOM to simulate the inundation process over Apponagansett Bay and Clarks Cover under an extreme weather condition of a hundred-year storm and then to assess the potential impact of climate change on the future flooding by taking the sea level rise (SLR) into account. The inundation map for the cases with 0.0-6.0 feet of SLR was created. This map was delivered to the Dartmouth Town for the purpose of guiding the coastal development planning along the Dartmouth coast. To understand the impact of the current-wave interaction on the coastal inundation in these two regions, we also conducted the numerical experiments for the cases with and without the inclusion of wave-current coupling. The results show that the wave-current interaction can enhance the onshore water transport, thus increase the surge level and cause much stronger flooding.

1. Introduction

1.1 Background

Coastal inundation is defined as flooding of normally dry land caused generally by some combination of heavy rains, high river discharge, tides, wind waves, storm surges, and tsunami wave trains. Hurricanes (tropical cyclones) and nor'easters (extratropical cyclones) are two major storm systems for flood risk along the Massachusetts coast. Serious coastal inundation usually happens when combined wind waves and storm surges coincide with high tides (Bernier and Thompson, 2006; Chen et al., 2013, Beardsley et al., 2013). For example, the August 18-19 1991 Hurricane Bob-generated strong winds (> 40 m/s), high storm surges, and heavy rains that caused extensive damage over New England, with a total loss of $1.5 billion in economic loss (Mayfield, 1992; Vallee and Dion, 2005). Hurricane Sandy swept over the US northeast region on October 28-29 2012, with wind guests above 37 m/s over Cape Cod and Buzzards Bay, MA. With its unusual merging with an air frontal system, "Superstorm Sandy" caused serious flooding along the New England coast and led to an economic loss of ~ $75 billion, including property damage, widespread power outages, subway shutdown in cities, and the closing of many businesses in the region (Blake et al., 2013, USA Today-October 30, 2012).

In Massachusetts, coastal inundation and damage are frequently caused by nor'easters and much less frequently by tropical cyclones. The October 1991 extratropical cyclone ("Perfect Storm" or "Halloween Nor'easter of 1991") produced strong winds (peak gusts above 27 m/s) and 8-m waves during high tides (1.2 m above normal), causing serious coastal flooding in eastern Massachusetts (esp. Cape Ann to Nantucket), with damage of ~$100M (seven counties declared Federal Disaster counties) (McCown, 2008). The December 27 2010 nor'easter (Freedman, 2010) produced sustained peak winds above 23 m/s and 6-m waves above high tides off Scituate, a coastal town located about 25 km southeast of Boston. The combination of high wind-driven along-shore currents and waves peaking near high tide caused serious flooding on both the North Shore (e.g. Rockport) and South Shore (e.g. Scituate) (Beardsley et al., 2013). Many houses lost power and were damaged, and parts of the primary sea wall were breached. The recent February 8-9 2013 nor'easter ('Blizzard of 2013"), a super winter storm formed by the merger of a warm moist Mid-Atlantic low and a cold northeast low, caused a snowfall of > 25 inches (0.6 m) and a storm surge of ~1.3-1.5 m in the Boston area (Freedman, 2013). The governor of Massachusetts declared a "state of emergency" for the blizzard (CBS News-February 8, 2013), with an initial estimate of coastal and property damage and economic loss greater than past nor'easter events.

According to the Intergovernmental Panel on Climate Change (IPCC) 4th Assessment Report (IPCC, 2007), climate change shows a tendency that future tropical and extratropical storms will be more intense and storm-produced coastal inundation will likely worsen as a result of rapid sea level rise (SLR) in tropic and extratropical regions of the North Atlantic Ocean. SLR will continue as thermal expansion due to climate warming, rapid melting of ice sheets in the Arctic and Antarctic Oceans (Pritchard et al., 2012; Hellmer et al., 2012), and melting glaciers. Projected SLR estimated from global temperature warming will be in the

range of 0.2-0.5 m at 2050 and up to 1.0-2.0 m at the end of this century (Figure 1) (Sallenger et al., 2012). This value could be much higher due to more rapid melting of ice sheets in summer in Greenland and west Antarctic ice sheets (Rahmstorf, 2010). A recent assessment of the effect of SLR on predicted changes in the intensity and paths of hurricanes in the North Atlantic shows that New York City will experience significantly larger storm surges (Lin et al., 2012).

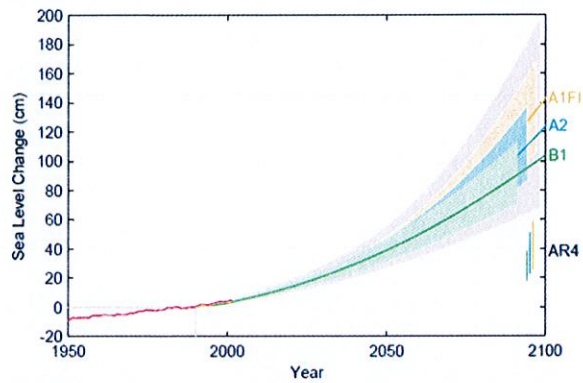

Figure 1. Projection of sea-level rise over 1995-2100 based on the IPCC temperature projection for three emission scenarios (B1, A2 and A1F1) (IPCC, 2007). Figure is downloaded from Vermeer and Rahmstorf (2009).

The Apponagansett Bay and Clarks Cove, Dartmouth, MA is located on the western coast of Buzzard Bay. This region was frequently influenced by storm-induced coastal inundation. The National Oceanic and Atmospheric Administration (NOAA) National Weather Service (NWS) Weather Forecast Offices (WFOs) in Taunton (MA) has identified 23 other coastal sites in Massachusetts that are "particularly vulnerable to extratropical flooding" and ten sites are in Buzzards Bay that are "most vulnerable" to extreme storm surge during hurricanes. With climate change scenarios predicting stronger storms and rising sea level, coastal flooding-induced hazards will directly affect local safety, marine and public activities, the coastal environment and economy.

1.2 Objectives

We, a joint team of UMASSD and WHOI, have developed the Northeast Coastal Ocean Forecast System (NECOFS) with support by NERACOOS and placed it into 24/7 forecast operations beginning in 2007. NECOFS has demonstrated the capability of forecasting weather, surface icing, surface waves, water level, ocean hydrographic (temperature and salinity) conditions, 3-D ocean currents, and storm-induced coastal inundation. The primary goal of this project is to provide an assessment of climate change on storm-induced flooding in Apponagansett Bay and Clarks Cove, Dartmouth Town, MA. The specific objectives of this project are to 1) develop a coastal inundation sub-grid model for Apponagansett Bay and Clark Cove and implement this into the NECOFS, 2) select a hundred-storm scenario to estimate the potential flooding in vulnerable areas, 3) for a given same hundred-year storm condition, re-conduct the experiment with considering the climate change induced sea level rise of 0 to 6 feet, respectively, and 4) create the potential flooding map in vulnerable areas under different climate change scenarios.

The technical requirements for the assessment of the impact of SLR on future storm-induced coastal inundation include: (1) a well-validated high-resolution, physical-based, unstructured-grid, coupled current-wave model with the capability of resolving the regional

and local seabed (water depth-bathymetry), land elevation (topography), complex irregular coastal geometry, as well as the flooding/drying process, wave-current interaction, refraction, radiation stress and wave run-up, (2) accurate enough river discharge, tidal forcing, and surface wind, pressure, and precipitation minus evaporation files to drive the coupled model system, and (3) successful simulation of tides and past nor'easters and hurricane-induced sea level changes and coastal inundations.

NECOFS meets the above technical requirements. The major outcome of our inundation model validation activities over the last five years is the success in building a model system that includes all key components. The basic FVCOM code includes the 3-D flooding/drying process (Chen et al, 2003, 2006a,b, 2007, 2013), which has been validated for wetland-estuarine-shelf water exchange in the Plum Island Sound-Merrimack River complex (Zhao et al., 2010) and tidal simulation in the Gulf of Maine and Massachusetts Bay (Chen et al., 2011). We have developed an unstructured-grid finite-volume version of the SWAN surface wave model (named "FVCOM-SWAVE) and implemented it into FVCOM. The coupled model has been validated by simulations of the surface waves in the Gulf of Maine (Qi et al., 2009), the Hurricane Bob storm surge over the New England shelf (Sun et al., 2013) and the 2005, 2007 and 2010 nor'easter-induced coastal inundation events in Scituate, MA (Beardsley et al., 2013, Chen et al., 2013).

2. Methods

2.1 A high-resolution DTC-FVCOM

Built on the success in establishing an "end-to-end" coastal inundation forecast model system under the framework of NECOFS, we have developed a high-resolution, subdomain coastal inundation model for the western Buzzard Bay coast, with the computational domain covering Apponagansett Bay and Clarks Cover (Figure 2). This subdomain inundation model was constructed using the unstructured grid Finite Volume Community Ocean Model (FVCOM), and named the Dartmouth Town Coastal FVCOM (abbreviated as "DTC-FVCOM"). The DTC-FVCOM was a coupled surface wave (FVCOM-SWAVE)/3-D ocean circulation model (FVCOM) system with built-in flooding/drying capability. FVCOM-SWAVE was implemented into FVCOM through the 3-D radiation stress approach (Mellor, 2003, 2005, 2008; Warmer et al., 2008). FVCOM is a prognostic, unstructured-grid, Finite-Volume, free-surface, 3-D primitive equation Community Ocean Model developed originally by Chen et al (2003) and has been improved by a team of UMASSD and WHOI researchers (Chen et al., 2004, 2006a, 2013). The equations are cast in a generalized terrain-following coordinate system with spatially variable vertical distribution (Pietrzak et al., 2002). The spatial fluxes of momentum are discretized using a second-order accurate finite-volume method (Kobayashi et al., 1999). A flux formulation for scalars (e.g. temperature, salinity) is used in conjunction with a vertical velocity adjustment to enforce exact local and global conservation of the scalar quantities. A Smagorinsky formulation (Smagorinsky, 1963) is used to parameterize the horizontal diffusion and turbulent vertical mixing is calculated using the

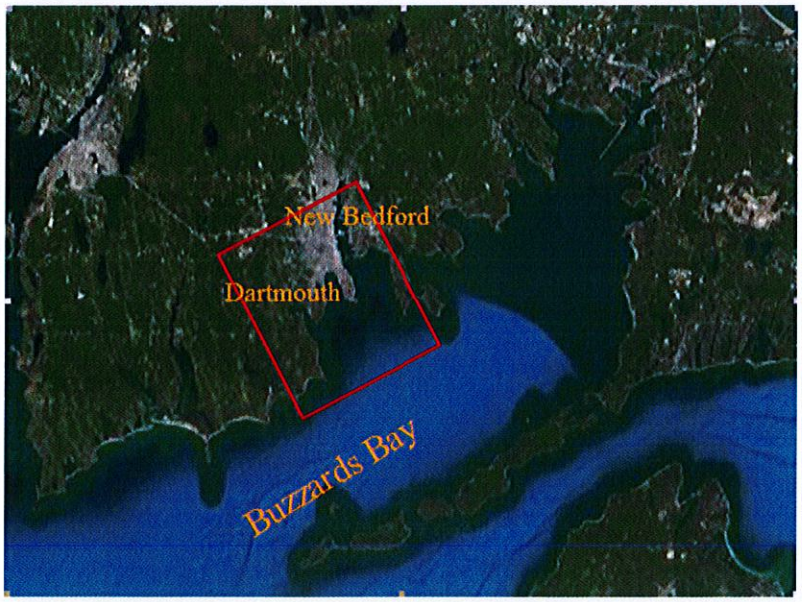

Figure 2. The location of the model domain. The region marked by a red color box is the computational domain of the DTC-FVCOM.

General Ocean Turbulence Model (GOTM) libraries (Burchard, 2002), with the 2.5 level Mellor-Yamada (1982) turbulence model used as the default. The ability of FVCOM to accurately solve scalar conservation equations combined with the topological flexibility provided by unstructured meshes makes it ideally suited for environmental prediction and interdisciplinary applications in coastal regions (see examples on http://fvcom.smast.umassd.edu).

2.1.1 Model grids

The computational domain of the DTC-FVCOM was configured with the unstructured triangles with a total node number of 44,956 and a total cell number of 89,717. The horizontal

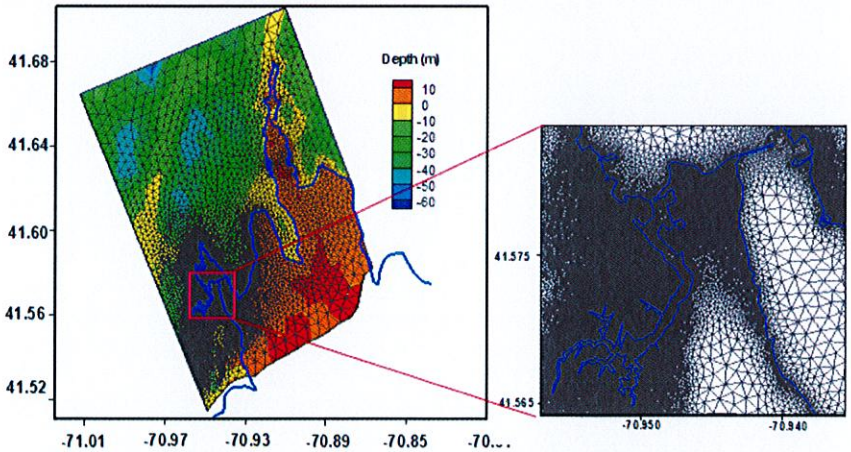

Figure 3. The unstructured triangular grid used for the DTC-FVCOM. The color image illustrated the water depth (positive for the water and negative for the land.

resolution was up to ~10 m. Six σ-levels (5 layers) with a uniform thickness was specified in the vertical, which produced a vertical resolution of 4 m on the 40-m isobath and up to ~ 0.5 m on the 5-m isobaths (Figure 3).

An effort was made to collect the high-resolution bathymetry in the Dartmouth coastal region. The bathymetry used in the DTC-FVCOM were from two sources. The Dartmouth Town provided us with the 1.0-m resolution USGS light detection and ranging (LiDAR) bathymetry data, which covered the Apponagansett Bay and Clarks Cover regions. In the area where the LiDAR was not available, we used the shuttle radar topography mission (STRM) data, which had a horizontal resolution of ~30 m.

2.1.2 Forcing and boundary conditions

The DTC-FVCOM was fully current-wave coupled hydrodynamic model driven by the surface wind stress with lateral boundary conditions specified using the tidal and non-tidal elevations plus significant wave height, direction and peak frequency. There was neither a tidal gauge nor a meteorological surface buoy for monitoring the water elevation, wind and surface waves in Apponagansett Bay and Clarks Cove. The tidal elevations on the boundary, the wind forcing at the sea surface, and significant wave height/direction/peak frequency were provided by the reanalysis results of NECOFS.

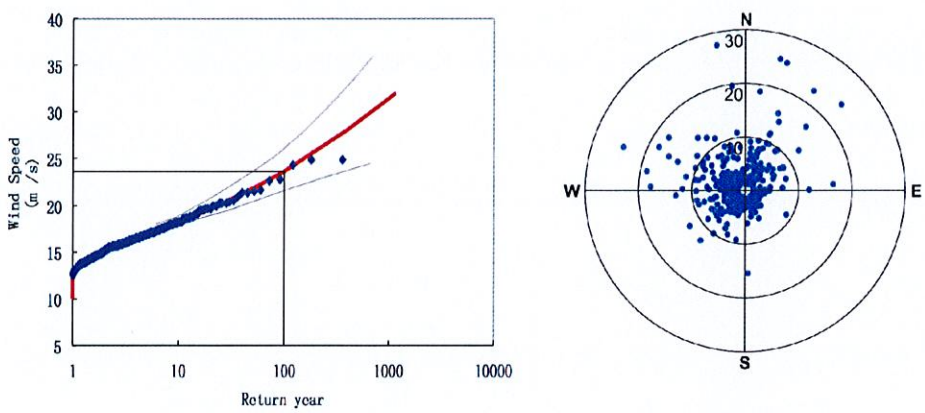

Figure 4. Left: Wind speed versus the storm return year. Dots: storm data samples; red curve: the extremal wind curve; grey curves: the 95% confidence internals. Right: Distributions of wind directions for individual storms. Labels "E, S, W and N" present the east, south, west and north directions, respectively. The wind direction was defined as the direction at which the wind blew from. The numbers on each axis were the wind speed. Analysis was done with 364 storm samples.

The hundred-year storm wind was determined by the statistical storm analysis of the wind field produced by the meso-scale weather model (named "WRF") in NECOFS. The storm was defined according to the magnitude and duration of the wind stress. When the local wind exceeded 0.2 Pa (25 mph) and lasted at least for 6 hours, we defined it as a storm. Over the 39-year period from 1978 to 2016, there was a total of 364 storms that struck Buzzard Bay. The

extreme wind speed for a hundred-year storm was 24 m/s (53.7 mph) (Figure 4), blowing predominantly from the northeast direction. A constant wind speed of 24 m/s, which represented the wind intensity of the hundred-year storm, was specified for the numerical simulation.

To assess the impact of sea level rise on possible maximum flooding, we considered a spring tidal condition. The NECOFS product included the hourly water elevation over the 39-year period from 1978 to 2016. We selected a point closed to Apponagansett Bay and conducted the harmonic analysis for the water elevation. The resulting magnitude of the tidal elevation in Apponagansett Bay during a spring tide cycle was 0.65 m (2.13 feet). The tidal forcing on the boundary was specified using a semi-diurnal M_2 tidal constituent with a magnitude of 0.65 m, which considered the maximum tidal elevation occurring during the spring tidal cycle.

The significant wave height and peak frequency were estimated based on the NECOFS-predicted surface waves in Buzzard Bay. In August 1991, Buzzard Bay was attacked by Hurricane Bob. Based on our simulation results, we found that the maximum surface wave height could reach 3.0 meter (m), with a peak period of 10 second (s) in Buzzard Bay. To take the extreme condition into account, we specified a significant wave height of 3.0 m at a peak period of 10 s as the forcing of surface waves on the boundary. In all simulations with inclusion of surface waves, the surface wave propagated onshore.

2.1.3 Design of numerical experiments

To provide a more objective assessment on the impact of climate-induced rise level rise on the potential coastal inundation in Apponagansett Bay and Clarks Cove, we conducted the experiments under different physical conditions. A total of 22 cases were selected to run the model, with detailed descriptions summarized in Table 1.

Table 1. The list of the forcing used in the 13 experiments

Fully wave-current coupled experiments with no SLR					
Case	Winds	Waves	Tides	SLR (feet)	Description
1	Yes	Yes	Yes	0	Northeasterly wind
2	Yes	Yes	Yes	0	Northerly wind
3	Yes	Yes	Yes	0	Northwesterly wind
4	Yes	Yes	Yes	0	Easterly wind
5	Yes	Yes	Yes	0	Southerly wind
6	Yes	Yes	Yes	0	Southeasterly wind
Fully wave-current coupled experiments with SLR					
Case	Winds	Waves	Tides	SLR (feet)	Description
7	Yes	Yes	Yes	1.0	Northeasterly wind
8	Yes	Yes	Yes	2.0	Northeasterly wind
9	Yes	Yes	Yes	3.0	Northeasterly wind

10	Yes	Yes	Yes	4.0	Northeasterly wind
11	Yes	Yes	Yes	5.0	Northeasterly wind
12	Yes	Yes	Yes	6.0	Northeasterly wind
13	Yes	Yes	Yes	1.0	Southeasterly wind
14	Yes	Yes	Yes	2.0	Southeasterly wind
15	Yes	Yes	Yes	3.0	Southeasterly wind
16	Yes	Yes	Yes	4.0	Southeasterly wind
17	Yes	Yes	Yes	5.0	Southeasterly wind
18	Yes	Yes	Yes	6.0	Southeasterly wind
Process-oriented experiments					
Case	Winds	Waves	Tides	SLR	Description
19	No	Yes	No	0	Only waves
20	No	No	Yes	0	Only tides
21	No	Yes	Yes	0	Tidal and wave, but no winds
22	Yes	No	Yes	0	Tide plus southeasterly wind, but no waves

The first experiment was made for the hundred-year storm case with no sea level rise (Case 1). In this case, a northeasterly wind was specified. To ensure that the model captures the most worse flooding situation, we also ran the model with the same wind amplitude but different wind directions. Case 2-6 represented for experiments with northerly, northwesterly, easterly, southerly and southeasterly winds. We found that for given same condition of tidal and wave forcings on the boundary, the southeasterly wind could cause relatively larger flooding in Apponagansett Bay and Clarks Cove. Although in the historic wind data, the occurrence frequency of southeasterly wind was very low, it might be possible when a hurricane attacks Buzzard Bay. For this reason, we selected the cases with northeasterly (hundred-year nor'easter storm) and southeasterly (possible a hurricane) winds as two representatives for our analysis.

Experiments with SLR were made for the cases with northeasterly and southeasterly winds, respectively. In each case, we re-ran the fully wave-current coupled model with 1.0-6.0 feet of SLR, respectively (Cases 7-12: northeasterly wind; Case 13-18: southeasterly wind). These cases were designed to assess the impact of climate change-induced sea level rise on the possible future storm-induced flooding in the region.

To evaluate the model performance under the different forcing conditions, we made 4 additional experiments to run the model with only wave forcing (Case 19), only tidal forcing (Case 20), tidal plus wave forcing (Case 21) and wind plus tidal forcing (Case 22), respectively.

All experiments were made over a two-day period. The tidal elevation reached an equilibrium state after half a day, while the wind and wave forcing was spin up over a tidal cycle. The maximum flooding occurred at the high tide after spin up time. The model output at the second-high tide on the second model-run day were used to draw the flooding map.

3. Results

The results described here are focused on the inundation maps produced by the cases with the hundred-year nor'easter northeasterly wind and the possible hurricane-produced southeasterly wind. The inundation maps were created for the assessment of climate vulnerability on potential flooding in the cases with 0, 1, 2, 3, 5, and 6 feet of SLR. The model-simulated waves and currents for the cases with 0 and 6 feet of SLR were compared to help understand why SLR could enhance the flooding in Apponagansett Bay and over the western coast of Clarks Cove.

3.1 Inundation maps

The model-predicted, storm-induced flooding is illustrated using the inundation map in Figure 5, with zoom-in views on two selected areas along the southeastern coast of Apponagansett Bay and the western coast of Clarks Cove in Figures 7 and 8, respectively.

Northeasterly wind **Southeasterly wind**

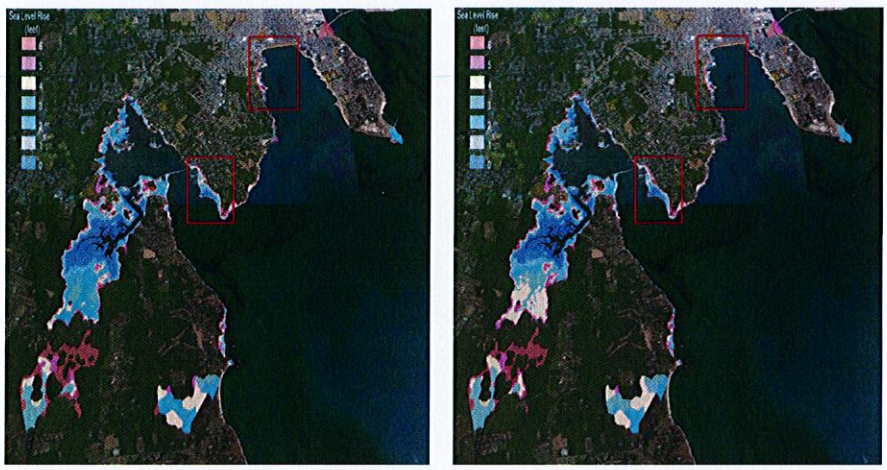

Figure 5: The inundation map of possible flooding in Apponagansett Bay and Clarks Cove for the cases with 0.0-6.0 feet of SLR under the northeasterly (left) and southeasterly (right) wind conditions, respectively. The red rectangle box in the right panel is the area where the zoom-in map was drawn.

Table 2: Possible flooding areas for the case with northeasterly wind

Case	Flooding areas (km^2)	Enlargement (%)	SLR	Description
1	1.34	0	0.0	Northeasterly wind
7	2.14	60	1.0	Northeasterly wind
8	3.07	129	2.0	Northeasterly wind
9	3.69	175	3.0	Northeasterly wind
10	4.72	252	4.0	Northeasterly wind
11	5.62	319	5.0	Northeasterly wind
12	6.78	506	6.0	Northeasterly wind

Note: The area enlargement rate is estimated relative to the flooding area with 0.0 feet of SLR.

Table 3: Possible flooding areas for the case with southeasterly wind

Case	Flooding areas (km^2)	Enlargement (%)	SLR (feet)	Description
6	1.45	0	0.0	Southeasterly wind
13	2.14	48	1.0	Southeasterly wind
14	2.81	94	2.0	Southeasterly wind
15	3.69	154	3.0	Southeasterly wind
16	4.86	235	4.0	Southeasterly wind
17	5.92	308	5.0	Southeasterly wind
18	7.11	390	6.0	Southeasterly wind

Note: The area enlargement rate is estimated relative to the flooding area with 0.0 feet of SLR.

For the case with the northeasterly wind, under the same hundred-year nor'easter storm condition, the climate-induced SLR could significantly enlarge possible flooding. In this case, the percentage rate of the area enlargement is approximately 60% per foot of SLR (Table 2; Figure 6). When the SLR reaches 6 feet, the flooding area could enlarge by 506% relative to the flooding area with 0.0 feet of SLR. This enlargement rate is much higher than the linear increase rate found for the cases with 1.0-5.0 feet of SLR. Compared with the case with northeasterly wind, the southeasterly wind produced a relatively larger flooding area: 8% larger. In this case, the percentage rate of the area enlargement is around 48% per foot of SLR (Table 3; Figure 6). This suggests that for the given intensity of an extratropical (nor'easter) or tropical (hurricane) storm, the impact of SLR is higher in the case with northeasterly wind.

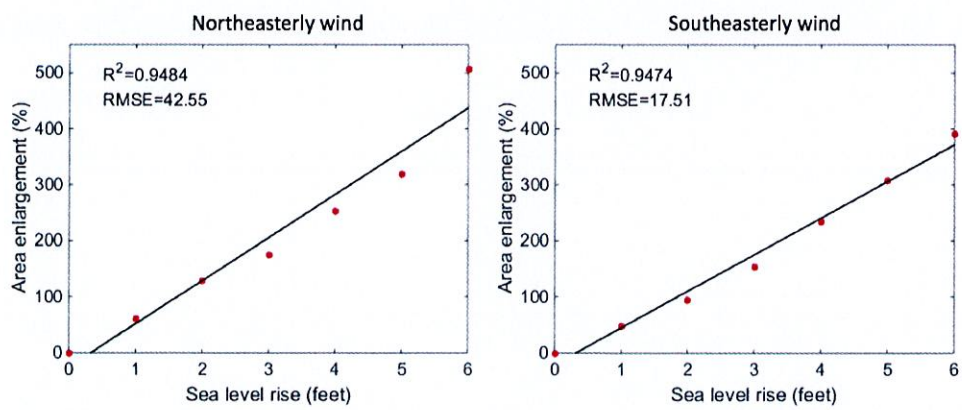

Figure 6: Percentage rate of flooding-area enlargement with the SLR for the cases with northeasterly (left) and southeasterly (right) winds.

The enlarged view of possible flooding area along the southeastern coast of Padanaram is given in Figure 7. Given the same intensity of a hundred-year storm, flooding along the southeastern coast on the south of the Apponagansett Bay bridge was similar in the cases with northeasterly and southeasterly winds. For a worse situation with 6.0 feet of SLR, the water could across Elm Street in Padanaram, South Dartmouth and houses on the beachside of Ricketson Point could be at risk to be flooded. It should be pointed out here that our estimation did not count the wave runup-induced splashing or overtop, which could be significant and

could be intensified with SLR during the southeasterly wind period. The view of possible

Northeasterly wind **Southeasterly wind**

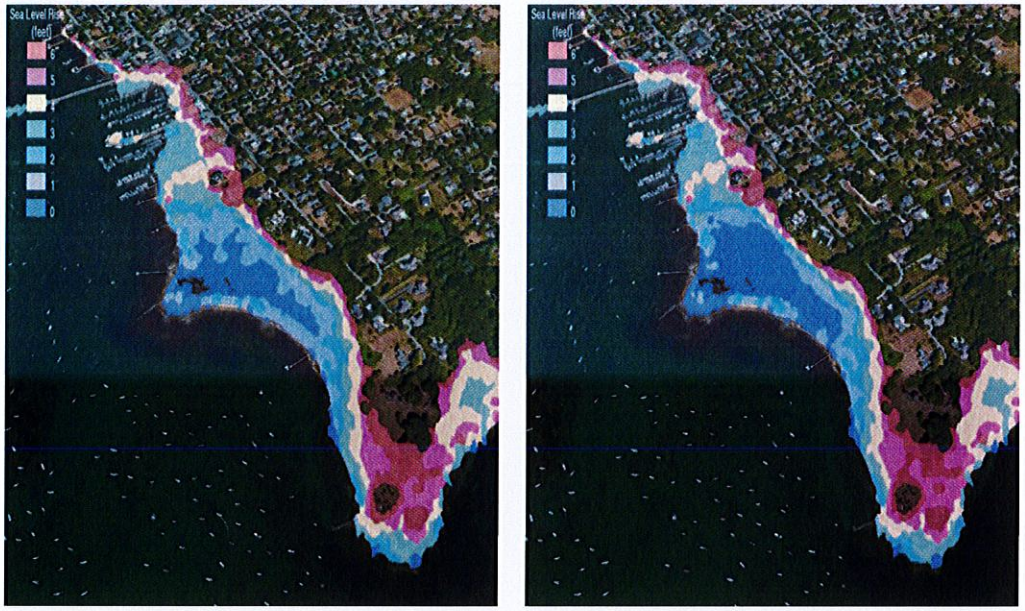

Figure 7: Enlarged view of possible flooding areas in the Padanaram coast for the cases with 0.0-6.0 feet of SLR under the given northeasterly (left) and southeasterly (right) wind conditions.

Northeasterly wind **Southeasterly wind**

Figure 8: Enlarged view of possible flooding areas in the Clarks Cove coast or the cases with 0.0-6.0 feet of SLR under the given northeasterly (left) and southeasterly (right) wind conditions.

flooding region can be viewed in the Google Earth map created using the model output (see the deliverable section).

The enlarged view of the possible flooding area along the northern and western coast of Clarks Cove is given in Figure 8. We can see that the seawall on the northern coast will function well to protect the city from storm-induced flooding, even in the case with 6.0 feet of SLR. However, on the western coast of Clarks Cove, a coast without the seawall, could be significantly influenced by the SLR. For the case with 6.0 feet of SLR, for example, the seawater could across Padanaram Ave and Marianna Street during both northeasterly and southeasterly wind periods. The flooding could be more worse during the northeasterly wind preriod.

3.2 Discussions

Taking the southeasterly wind case as an example, we examined the change of storm-induced surface waves and currents after SLR. Under the given same condition of tidal and wave forcings on the boundary and wind forcing at the sea surface, the surface wave could

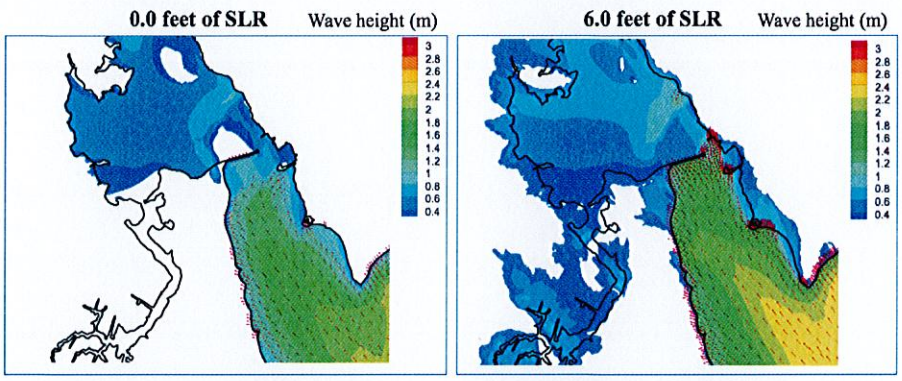

Figure 9: Comparison of the significant wave height at the high tide under the southeasterly wind period for the cases with 0.0 (left) and 6.0 (right) feet of SLR.

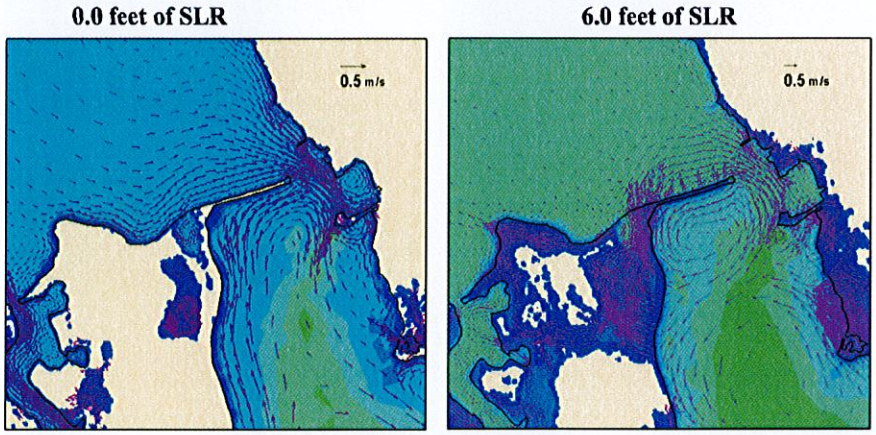

Figure 10: Comparison of the velocity vector fields at the high tide under the southeasterly wind period for the cases with 0.0 (left) and 6.0 (right) feet of SLR.

become much stronger as the sea level rises. For the case with 6.0 feet of SLR, the significant wave height could increase by ~3 feet (Figure 9). This means that under the same storm condition, we will expect much strong surface waves in the southern area of the Apponagansett Bay on the seaside of the bridge. Correspondingly, the current can become much stronger, forming the two-eddy flow in the southern area: anticyclonic close to the bridge and cyclonic in the down southern region (Figure 10). These two eddies push the water towards the western coast, which can significantly enhance flooding over that area. Although we did not count the flooding due to the wave runup in our experiments, it is clear that the Apponagansett Bay bridge will face a more serious attack by the storm-indued surface waves as the sea level rises. As a result of the intensification of the surface waves, the current-wave interaction could cause a much stronger flow toward the bridge, and hence enhance flooding.

4. Deliverable data

The deliverable data include the inundation maps for the cases with 0.0-6.0 feet of SLR under the northeasterly and southeasterly wind conditions. To provide a clear view, we have merged all inundation maps into the Google Earth. Two files enclosed in this report are 1) *btm_NE_WIND_result.kmz* and 2) *SE_WIND_result.kmz*. These two files are opened using Google Earth or Google Earth Pro.

Conclusions

A coastal inundation sub-grid FVCOM model was developed with a computational domain covering Apponagansett Bay and Clark Cove. The analysis was conducted to define a hundred-year storm, which was selected as the extreme storm scenario to assess potential flooding in the vulnerable areas. The numerical experiments were made for a given hundred-year storm with consideration of the climate change induced SLR of 0.0-6.0 feet, respectively, and the inundation maps for potential flooding in the vulnerable areas under different climate change scenarios were created.

The numerical experiments were made with inclusion of the wave-current interaction under the spring tidal condition. The hundred-year storm wind was determined by the statistical storm analysis of the wind field data produced by WRF in NECOFS. Over the 39-year period from 1978 to 2016, there were a total of 364 storms that struck Buzzard Bay. The extreme wind speed for a hundred-year storm was 24 m/s (53.7 mph), blowing predominantly from the northeasterly direction. The harmonic analysis was conducted for NECOFS-produced 39-year hourly water elevation, and the resulting maximum magnitude of the tidal elevation in Apponagansett Bay during a spring tide cycle was 0.65 m (2.13 feet). The surface wave forcing, with significant height of 3.0 m (9.84 feet) and a peak period of 10 sec, on the boundary was specified based on NECOFS-simulated wave field in Buzzard Bay for the August 1991 Hurricane Bob.

The DTC-FVCOM experiments were first made for the case with the northeasterly wind condition and repeated by the change of the wind direction. According to the model-predicted flooding area, we found both northeasterly and southeasterly winds could produce the large

coastal inundation in Apponagansett Bay and Clark Cove. Since a strong southeasterly wind could possible occur when a hurricane attacks this region, the assessment for the potential impact of climate change-induced sea level rise on the future flooding was conducted for both northeasterly and southeasterly wind cases.

The inundation maps for the cases with 0.0-6.0 feet of SLR were created using the Google Earth. The results suggest that the storm could cause a large flooding in Apponagansett Bay and Clark Cove as a result of SLR. For the given same intensity of a hundred-year storm, as the sea level rises, the southeastern coast of Apponagansett Bay and the western coast of Clark Cove could be risk for storm-induced flooding. The project produced two Google Earth files for inundation maps for the cases with 0.0-6.0 feet of SLR under the northeasterly and southeasterly wind conditions.

References

Beardsley, R. C., C. Chen and Q. Xu, 2013. Coastal flooding in Scituate (MA): a FVCOM study of the Dec. 27, nor'easter. *J. Geophys. Res.*, 118, doi: 10.1002/2013JC008862.

Bernier, N. and K.R. Thompson, 2006. Predicting the Frequency of Storm Surges and Extreme Sea Levels in the Northwest Atlantic. *J. Geophys. Res.*, 111, C10009, doi:10.1029/2005JC003168.

Blake, E. S; T. B. Kimberlain, R. J. Berg, J. P. Cangialosi and J. L. Beven II, 2013. Hurricane Sandy: October 22 – 29, 2012, Tropical Cyclone Report, (February 12, 2013), National Hurricane Center, United States National Oceanic and Atmospheric Administration's National Weather Service.

Burchard, H., 2002. Applied turbulence modeling in marine waters. Springer:Berlin-Heidelberg-New York-Barcelona-Hong Kong-London-Milan Paris-Tokyo, 215pp.

CBS-February 8, 2013 News: http://boston.cbslocal.com/2013/02/08/patrick-declares-state-of-emergency-announces-travel-ban-in-mass/.

Chen, C., H. Liu, and R. Beardsley, 2003. An unstructured grid, finite-volume, three-dimensional, primitive equations ocean model: Application to coastal ocean and estuaries. *J. Atm. & Ocean Tech.*, 20 (1), 159–186.

Chen, C, G. Cowles and R. C. Beardsley, 2004. An unstructured grid, finite-volume coastal ocean model: FVCOM User Manual, SMAST/UMASSD Technical Report-04-0601, pp183.

Chen, C, R. C. Beardsley and G. Cowles, 2006a. An unstructured grid, finite-volume coastal ocean model (FVCOM) system. Special Issue entitled "*Advance in Computational Oceanography*", *Oceanography*, 19(1), 78-89.

Chen, C., R.C. Beardsley, and G. Cowles, 2006b, An unstructured grid, finite-volume coastal ocean model-FVCOM user manual, School for Marine Science and Technology, University of Massachusetts Dartmouth, New Bedford, Second Edition. Technical Report SMAST/UMASSD-06-0602, 318pp.

Chen, C. H. Huang, R. C. Beardsley, H. Liu, Q. Xu and G. Cowles, 2007. A finite-volume numerical approach for coastal ocean circulation studies: comparisons with finite

difference models. *J. Geophys. Res.* 112, C03018, doi:10.1029/2006JC003485.

Chen, C., H. Huang, R. C. Beardsley, Q. Xu, R. Limeburner, G. W. Cowles, Y. Sun, J. Qi, and H. Lin, 2011. Tidal dynamics in the Gulf of Maine and New England Shelf: An application of FVCOM. *J. Geophys. R*es., 116, C12010, doi:10.1029/2011JC007054.

Chen, C. R. C. Beardsley, R. A Luettich Jr, J. J. Westerink, H. Wang, W. Perrie, Q. Xu, A. S. Dohahue, J. Qi, H. Lin, L. Zhao, P. Kerr, Y. Meng and B. Toulany, 2013. IOOS/SURA Extratropical Storm Inundation Testbed: Inter-model (ADCIRC, FVCOM and SELFE) comparisons in Scituate, Massachusetts. *J. Geophys. Res.*, 118, doi:10.1002/jgrc.20397.

Chen, C., R. C. Beardsley, G. Cowles, J. Qi, Z. Lai, G. Gao, D. Stuebe, H. Liu, Q. Xu, P. Xue, J. Ge, R. Ji, S. Hu, R. Tian, H. Huang, L. Wu, H. Lin, Y. Sun and L. Zhao, 2013. An unstructured-grid, finite-volume community ocean model FVCOM user manual (3rd edition), SMAST/UMASSD Technical Report-13-0701, University of Massachusetts-Dartmouth, pp 404.

Freedman, A., 2013. Blizzard of 2013 brings another threat: coastal flooding, Climate Central News published on February 8, 2013.

Hellmer, H. H., F. Kauker, R. Timmermann, J. Determann and J. Rae, 2012. Twenty-first-century warming of a large Antarctic ice-shelf cavity by a redirected coastal current. *Nature*, 485, 225-228.

IPCC, 2007: Climate Change 2007: The Physical Science Basis. Contribution of Working Group I to the Fourth Assessment Report of the Intergovernmental Panel on Climate Change [Solomon, S., D. Qin, M. Manning, Z. Chen, M. Marquis, K.B. Averyt, M. Ignore and H.L. Miller (eds.)]. Cambridge University Press, Cambridge, United Kingdom and New York, NY, USA.

Kobayashi, M. H., J. M. C. Pereira and J. C. F. Pereira, 1999. A conservative finite-volume second-order-accurate projection method on hybrid unstructured grids, *J. Comput. Phys.*, 150, 40-45.

Lin, N., K. Emanuel, M. Oppenheimer and E. Vanmarcke, 2012. Physical based assessment of hurricane surge threat under climate change, *Nature Climate Change*, 2, 462-467, doi: 10.1038/ncclimate1389

McCown, S, 2008. "Perfect Storm" Damage Summary". National Climatic Data Center. National Oceanic and Atmospheric Administration. http://www.ncdc.noaa.gov/oa /satellite/satelliteseye/cyclones/pfctstorm91/pfctstdam.html

Mellor, G. L. and T. Yamada, 1982. Development of a turbulence closure model for geophysical fluid problem. *Rev. Geophys. Space. Phys.*, 20, 851-875.

Pieterzak, J. J. B. Jakobson, H. Burchard, H. J. Vested, and O. Petersen, 2002. A three-dimensional hydrostatic model for coastal and ocean modeling usuing a generalized topography following co-ordinate system. *Ocean Modeling*, 4: 173-205.

Pritchard, H. D., S. R. M. Ligtenberg, H. A. Fricker, D. G. Vaughan, M. R. van den Broeke and L. Padman, 2012. Antarctic ice-sheet loss driven by basal melting of ice shelves. *Nature*, 484, 502-505.

Qi, J., C. Chen, R. C. Beardsley, W. Perrie, Z. Lai and G. Cowles, 2009. An unstructured-grid finite-volume surface wave model (FVCOM-SWAVE): implementation, validations and applications. *Ocean Modelling*, 28, 153-166. doi:10.1016/j.ocemod. 2009.01.007.

Rahmstorf, S., 2010. A new view on sea level rise, Nature, 4, 44-45.

Sallenger, A. H. Jr., K. S. Doran and P. A. Howd, 2012, *Nature Climate C*hange, 2, 884-888, doi:10.1038/ncclimarte1597.

Smagorinsky, J., 1963. General circulation experiments with the primitive equations, I. The basic experiment *Monthly Weather Review*, 91, 99–164.

Sun, Y., C. Chen, R. C. Beardsley, Q. Xu, J. Qi and H. Lin, 2013. Impact of current-wave interaction on storm surge simulation: a case study for Hurricane Bob. *J. Geophys. Res.*, 118, 2685-2701, doi:10.1002/jgrc.20207

USA Today-30-October 2012. Sandy leaves millions without power: 15 dead.

Vallee, D. R. and M. R. Dion, 2005. Hurricane Bob, Boston, MA National Weather Service, Retrieved 2011-07-12.

Zhao, L., C. Chen, J. Vallino, C. Hopkinson, R. C. Beardsley, H. Lin and J. Lerczak, 2010. Wetland-estuarine-shelf interactions in the Plum Island Sound and Merrimack River in the Massachusetts coast. *J. Geophys. Res.*, 115, C10039, doi:10.1029/2009JC006085.